NUMERICAL ANALYSIS OF HEADED STUDS EMBEDDED IN LARGE PLAIN CONCRETE BLOCKS

J.Ožbolt and R.Eligehausen

Institut für Werkstoffe in Bauwesen
Universität Stuttgart

SUMMARY

Anchoring elements such as headed studs, expansion, grouted or undercut anchors are used for local transfer of loads into concrete members. Parameter study of the behavior of headed stud anchors with embedment depth h_v = 130 mm and failing by pulling out a concrete cone, is performed through numerical analysis. Compression and tension strength, fracture energy and the head diameter are varied. Numerical analysis is performed using nonlocal microplane model and axisymmetric finite elements. Results of the analysis are compared with experimental results.

1. INTRODUCTION

Provided the steel strength of the stud is high enough, headed studs embedded in a large concrete block subjected to tensile loading fail by pulling a cone out of the concrete. The circumferential crack forming this cone is generated and growing in a so-called mixed mode. In recent years several attempts have been made to understand this growth and to predict the pull-out load of headed studs [1-4]. Summarizing this activities it can be said that material models based on plasticity and on stress-strain relationships together with stress criteria indicating failure are not capable to predict behavior of anchors as observed in experiments [5]. Furthermore, the predicted failure load depends on the element size and load step size [6]. A better explanation of anchorage behavior can be expected using more general material models based on fracture mechanics. Therefore, a numerical analysis of a headed stud embedded in a large plain concrete block is carried out. Varied are the concrete properties and the size of anchor head. The analysis is based on axisymmetric

isoparametric four-node finite elements. As a material model, nonlocal microplane model for concrete is used. The microplane model takes into account microstructural stress-strain interaction between orientations, while concept of nonlocal continuum takes fracture mechanics into account by considering interactions over a distance.

2. REVIEW OF THE NONLOCAL MICROPLANE MODEL

The basic idea of the microplane models, which is due to Taylor [7], was initially applied only to metal plasticity and went under the name "slip theory". Extension to nonsoftening behavior of rocks and soils were made in [8]. To make the Taylor's idea applicable to strain-softening brittle behavior, some major conceptual modifications were needed [9]. Most recently the concept was extended to strain-softening brittle-plastic behavior, typical of concrete, [10]. This latest formulation provides a very complete material model for concrete under tensile as well as compressive triaxial stress states. Since the deformation on various planes in the microstructure could no longer be called "plastic slip", the more general term "microplane" was coined [9]. According to the microplane model hypothesis [10], the behavior on the microplane level can be described by nontensorial path-independent total stress-strain relations of the form:

$$\sigma_V = F_V(\varepsilon_V), \quad \sigma_D = F_D(\varepsilon_D), \quad \sigma_T = F_T(\varepsilon_T) \qquad (1)$$

where, subscripts V, D and T stays for volumetric, deviatoric and shear component on the microplane. For two reasons, namely representation of unloading and application of the nonlocal damage concept, it is convenient to have the total stress-strain relation in the form of continuum damage mechanics:

$$\sigma_V = C_V\varepsilon_V, \quad \sigma_D = C_D\varepsilon_D, \quad \sigma_T = C_T\varepsilon_T \qquad (2)$$

C_V, C_D and C_T represent secant modulus (volumetric, deviatoric and shear). This modulus is in the case of loading, except in the case of volumetric compression, an exponential function of total microplane strain (volumetric, deviatoric and shear). During unloading the secant modulus is taken as a constant and equal to the initial secant modulus.

Incremental macroscopic stress-strain is found from stress equilibrium between the micro- and macro-levels using virtual work approach, and efficient numerical integration over the sphere (21 integration points).

The main advantage of the microplane model is its generality and conceptual simplicity. The model can prescribe behavior of concrete in any stress-strain state using only a few material parameters. The material stiffness matrix is generally nonsymmetric and anisotropic.

In classical local continuum analysis by finite element method, strain localization endangers problems of instability, inobjectivity and spurious mesh sensitivity [6]. This problems are here avoided using the nonlocal continuum concept, where the material parameters, in the case of material damage, depend on nonlocal strains [11].

The analysis is performed with the computer program described in [12], which was developed by the first author. In this program, a constant stiffness approach is used, and nonlinearity is introduced through stress vector [12].

3. NUMERICAL ANALYSIS

A headed stud embedded in a large concrete block is analyzed using axisymmetric four-node isoparametric finite elements (Fig. 1). Pulling of the anchor is performed by prescribing displacements at the bottom of the stud. Contact between steel stud and concrete exists only under the head of

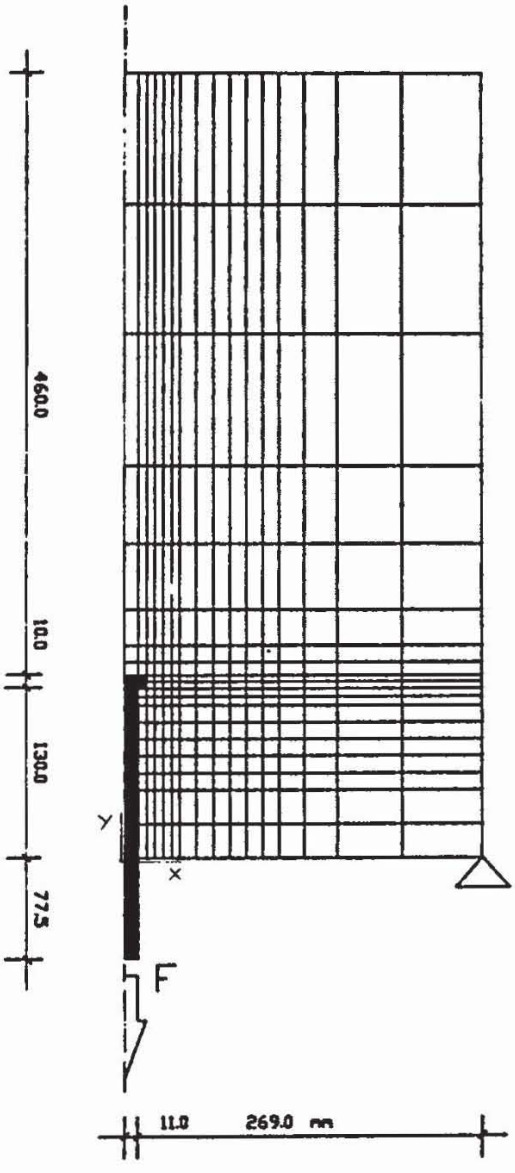

Fig. 1 Finite element mesh and geometry used in the analysis

the stud. To account for the restraining effect of the embedded anchor, the displacements of the concrete surface along the steel stud in the vicinity of the head are fixed in X-direction. The horizontal displacement of the support is fixed, and the concrete surface is supposed to be free.

In the analysis, the influence of the concrete properties as well as the influence of the size of the head on the anchor behavior is investigated. Concrete compression and tension strength, fracture energy of concrete and the size of the head are considered as parameters. In all examples the embedment depth (h_v = 130 mm) and the diameter of the steel bar (22 mm) are constant. Two slightly different finite element meshes are used, to analyze two head sizes of the anchor d= 35 and 52 mm. Results of the experiment are also available for the present geometry and material properties [13].

In the analysis, different concrete material properties are used. Young's modulus (E= 23500. MPa) and Poisson ratio (ν= 0.18) are constant in all examples and taken as in the experiment. Two different compression properties (Fig. 2) and three different tension properties are considered (Fig. 3). The given G_F values were calculated using a unit area finite element with length l= 360 mm, as in the experiment. According to [11], the characteristic length which defines the representative volume of the material is about 3 times the maximum aggregate size. Because only very small aggregates can be present under the head, the characteristic length is assumed as l= 6.0 mm. The value is identical with the size of the smallest finite element.

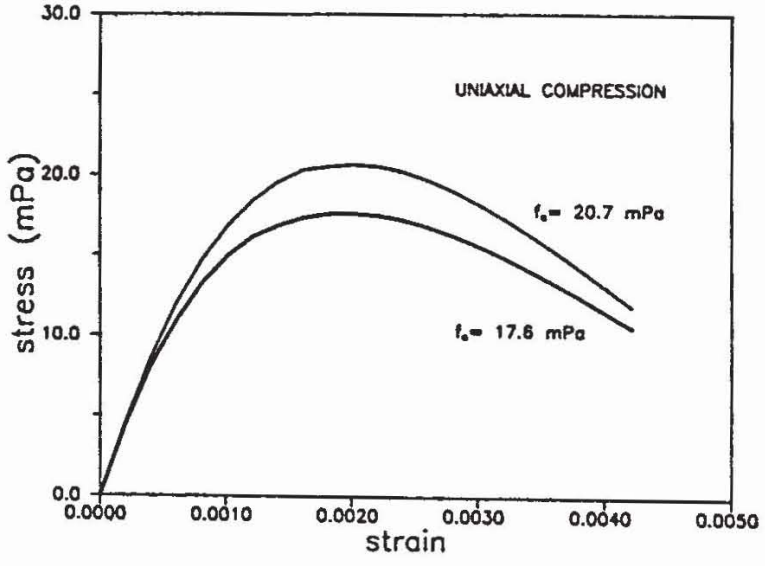

Fig. 2 Uniaxial compression stress-strain properties used in the analysis

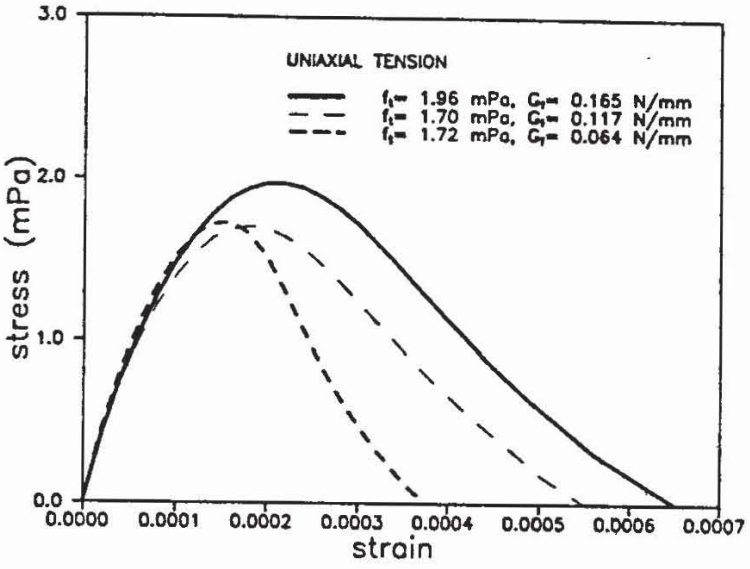

Fig. 3 Uniaxial tension stress-strain properties used in the analysis

4. RESULTS OF THE NUMERICAL ANALYSIS

To confirm that the microplane model can correctly prescribe behavior of plain concrete in a pull-out test the results of the numerical analysis are compared with the test results. Material parameters used in numerical analysis are similar as in the experiment. Uniaxial compression strength used is f_c = 17.6 MPa (in experiment 18.8), tension strength f_t = 1.72 MPa (1.80 in test) and fracture energy G_F = 0.064 N/mm (0.070 in test).

Calculated and measured failure load agree rather well (Fig. 4). While the calculated initial stiffness agrees well with the measured value, the displacements at failure are smaller than observed in the experiment. This is mainly influenced by the local behavior of concrete under the head (Fig. 5). It should be noted that the area of the anchor head is relatively small (d= 35 mm), and due to this the average compression stress under the head at failure load is about 10 times larger than the uniaxial compression strength f_c (the maximum calculated value in one integration point is $20^c f_c$). Therefore, most of displacements in the load displacement diagram (Fig. 4) is due to concrete compression softening under the anchor head. The concrete pre- and post-peak behavior under very high compression in 3D stress-strain state have to be correctly modelled to predict failure mode and displacement correctly. Obviously the assumed peak stress in the 3D -stress state is too high in comparism to the behavior found in the test. However, in general the calculated displacement field (Fig. 5) is in very good agreement with the experimental observation. According to [13], most of the total displacement

is due to concrete compaction under the anchor head.

Crack development at different load stages (25%, 60% and 100% of failure load) is shown in Fig. 6. While circumferential cracking starts relatively early at the anchor head and progresses towards the concrete surface, radial cracks are initiated at much higher loads at the surface. Failure is caused by circumferential cracking. Discrete crack direction and length of the circumferential crack at peak load (Fig. 6c) are reconstructed from the calculated maximum tensile strains. The calculated slope of the failure cone surface is in good agreement with experimentally measured results [13]. The average angle between the pulled cone surface area and the concrete surface amounts to about $\alpha = 35^{\circ}$.

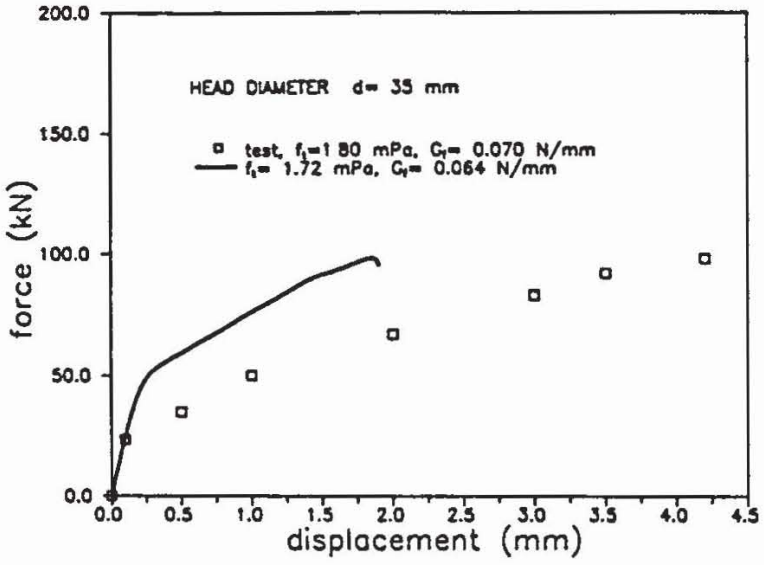

Fig. 4 Load-displacement curve - experiment and numerical analysis

In Fig. 7, the ratio between crack cone surface area and total crack cone surface area (calculated for $\alpha = 35^{\circ}$) is plotted. Stable crack growth starts at about 30% of the failure load and further crack growth is very stable up to the failure load, when unstable crack development starts. These results are again in good agreement with experimental observations based on measurements of concrete strains [13].

Summarizing, the failure of the analysed headed stud embedded in concrete is due to circumferential cracking of concrete, while the compression behavior of concrete under the head is mainly responsible for the displacement at failure.

In Fig. 8 the influence of the tensile strength f_t and fracture properties of concrete G_F on load displacement behavior is analysed. Three different properties for concrete in tension are considered (Fig. 3). The concrete compression properties are fixed, with uniaxial compression strength f_c = 17.6 MPa. Diameter of the anchor head is also constant (d= 35 mm). Fig. 8. clearly indicates strong dependency between fracture properties of concrete and failure load. Roughly, the

failure load is proportional to the square root of fracture energy (Fig. 9). This confirms analytical and experimental results obtained in [14].

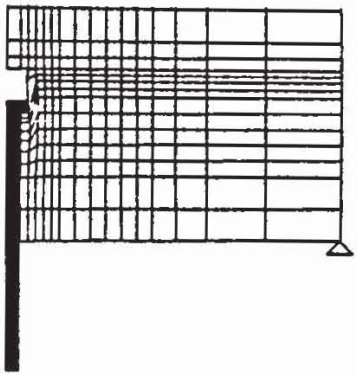

Fig. 5 Displacement field at peak load

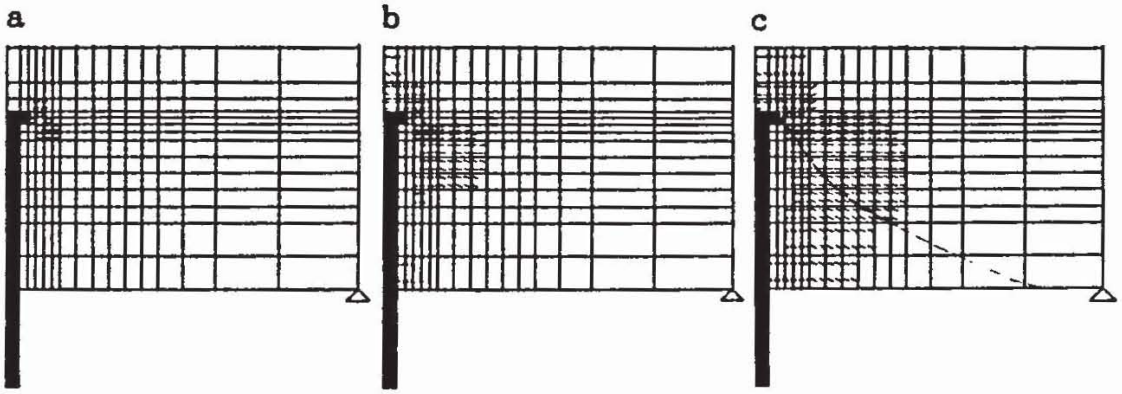

Fig. 6 Crack development at different load stages (25%, 60% and 100% of the peak load)

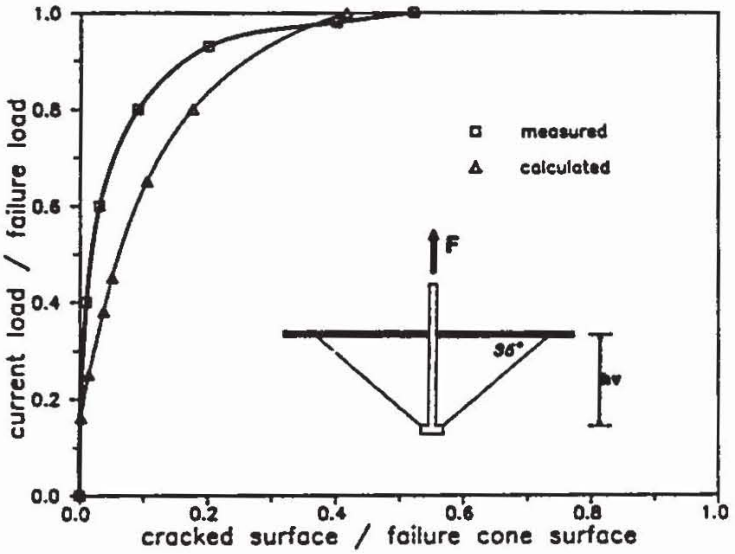

Fig. 7 Calculated and measured crack surface area

To demonstrate that the failure of specimen is not due to a compression failure of concrete under the head, two specimens with the same concrete properties but different head diameters (d= 35 and 52 mm) are compared. Results of this analysis (Fig. 10) demonstrate that, within the range of the assumed head diameters, the failure load does not depend significantly on concrete compression stress-strain state under the anchor head. Increasing the effective head area by a factor of 3, the increase of the calculated failure load is only 17 %. For a head diameter d= 52 mm the average compression stress under the head at failure is only about 3.75 f_c compared to 10 f_c for d= 35 mm. Due to this reduction of the compression stress, the displacement of the anchor head is much smaller (compare Fig.

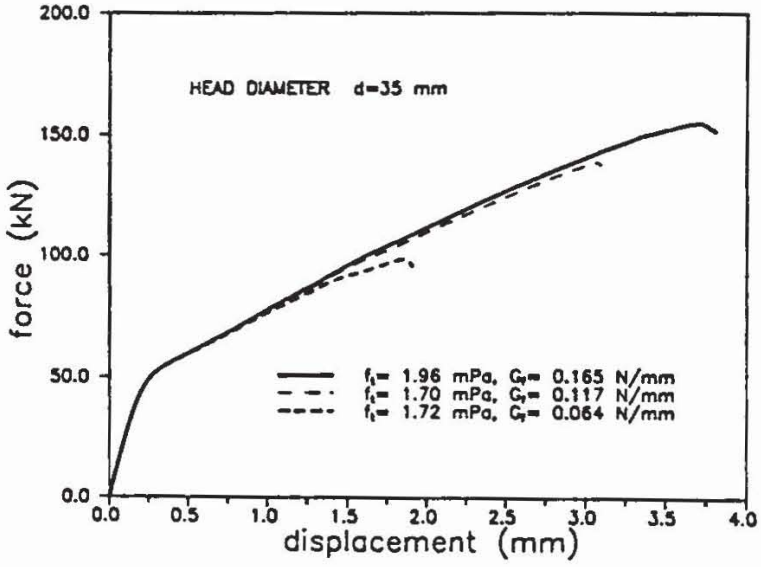

Fig. 8 Load-displacement diagram for three different fracture properties

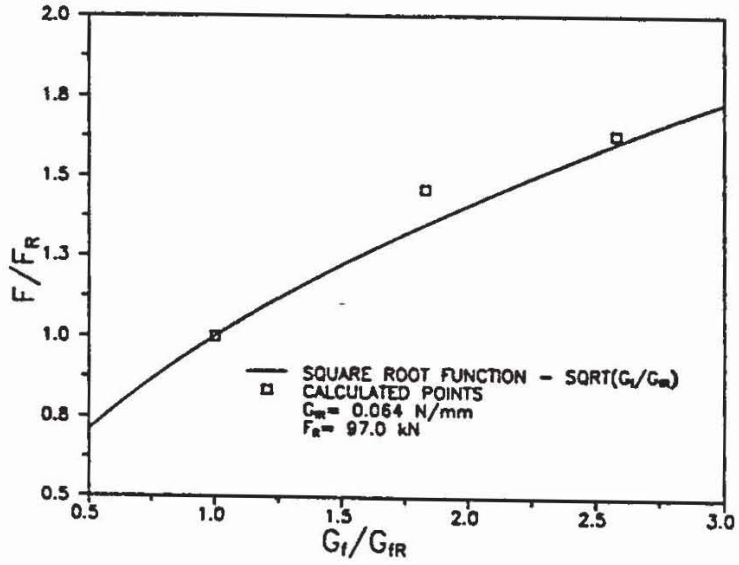

Fig. 9 Failure load as a function of fracture properties

11b and Fig. 5). Therefore with decreasing head diameter the concrete compression softening under the head contributes larger displacement at failure load. This numerical results are in agreement with test evidence [15].

For a anchor head diameter d<< 35 mm, the displacement of the anchor head will increase even more, reducing the actual embedment depth and thus the concrete cone failure load [16].

In Fig. 11, the crack development and displacement field at failure for an anchor with head diameter d= 52 mm are shown. In contrast to the smaller head size (d= 35 mm), average cone angle at failure is larger.

From the numerical point of view, analysis of the specimen with smaller head size, converges very slowly and requires considerably more computer time than analysis of the specimens with larger head size. This is a consequence of 3D compression softening.

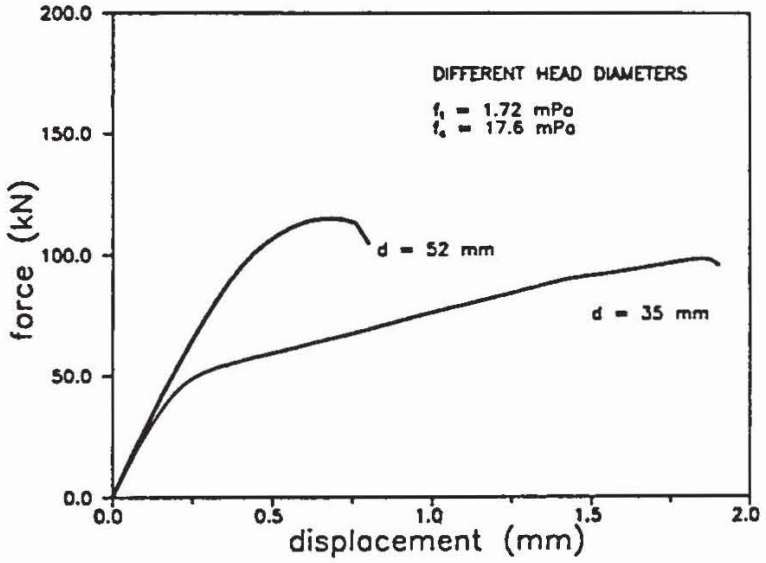

Fig. 10 Load-displacement curve for two different head diameters

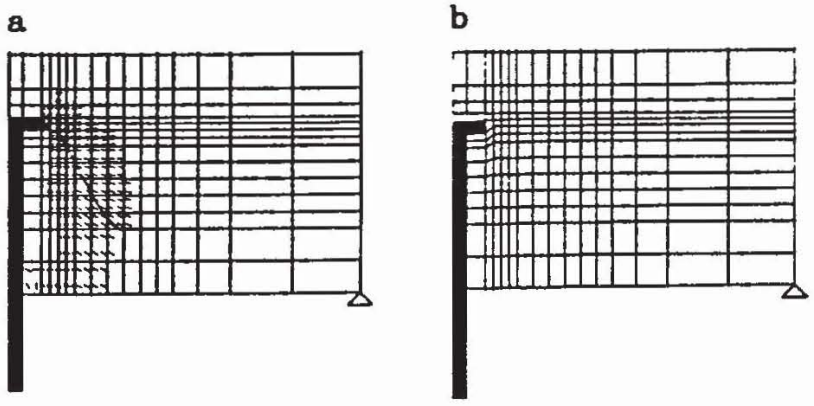

Fig. 11 Crack formation and displacement field at a peak load in the case of larger head diameter

The influence of concrete compression strength is demonstrated in Fig. 12, where the results of two specimens with head diameter d= 52 mm are presented. Tension strength and fracture properties of concrete are invariant, while two different concrete compression strengths are considered (Fig. 2). Results clearly indicate insensitivity of the failure load on concrete compression strength, but again displacement at failure is smaller if concrete compression strength is higher.

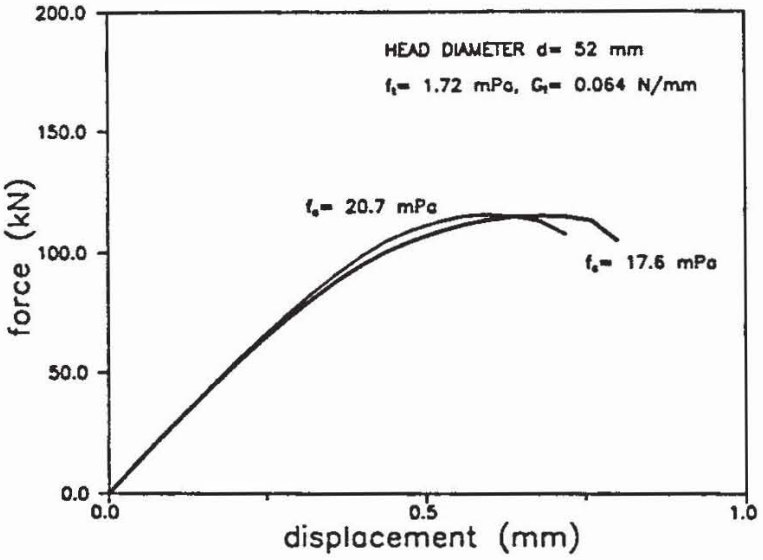

Fig. 12 Load-displacement diagram for two different concrete compression strength

5. CONCLUSION

The behavior of a headed stud (stud diameter 22 mm, head diameter d=35 and 52 mm) embedded in a large plain concrete block (embedment depth h_v = 130 mm) is analyzed using axisymetric isoparametric four-node finite elements and nonlocal microplane model. The numerical results are in good agreement with experimental observations. In all analyzed examples, failure is due to failure of concrete in tension (circumferential cracking) rather than in compression. Circumferential crack growth starts at about 30% of failure load and is very stable up to peak load. After the peak load unstable cracking develops and the final failure cone is formed. The fracture load is mainly influenced by the fracture energy of concrete G_F , and is approximately a square root function of G_F . The size of the anchor head as well as the properties of concrete in compression have a rather small influence on the failure load, however they influence the

load-displacement relationship significantly.

It should be noted that this conclusions are valid for the assumed range of the anchor geometry only. For more general conclusions, specimens with broader range of geometry variations should be tested and analyzed.

6. REFERENCES

1. Ottosen, N. S. - Nonlinear Finite Element Analysis of Pull-Out Tests. Journal of Structural Division, Vol. 107, No. ST4, pp. 591-603, 1981.

2. Eligehausen, R. and Sawade, G. - Behavior of Concrete in Tension. Betonwerk + Fertigteil Technik, No. 5 and 6, 1985.

3. Krenchel, H. and Shah, S. - Fracture Analysis of the Pull-Out Tests. Material and Structures, Vol. 108.

4. Ballarini, R.; Shah, S. and Keer, L. - Failure Characteristics of Short Anchor Bolts Embedded in a Brittle Material. Proc. R. Soc. London, A 404, pp. 35-54, 1986.

5. Eligehausen, R. and Sawade, G. - 'Analysis of Anchoring Behavior (Literature Review)', Fracture Mechanics of Concrete Structures - RILEM Report, Ed. L.Elfgren, Chapman and Hall, 1989, pp.263-280.

6. Cedolin, L. and Bazant, Z. P. - Effect of Finite Element Choice in Blunt Crack Band Analysis. Comp. Meth. in Appl. Mec. and Eng. 24, pp. 305-316, 1980.

7. Taylor, G.I. - Plastic Strain in Metals. Journal of Inst. of Metals, Vol. 62, pp. 307-324., 1938.

8. Zienkiewicz, O. C. and Pande, G. N. - Time dependent multi-laminate model of rock -- a numerical study of deformation and failure of rock. Int. Journal of Num. and Anal. Math. in Geomechanics 1, pp. 219-247, 1977.

9. Bazant, Z. P. and Gambarova, P. G. - Crack Shear in concrete: Crack Band Microplane Model. J. Struc. Eng., ASCE, 110(9), pp. 2015-2035., 1984.

10. Bazant, Z. P. and Prat P. C. - Microplane Model for Brittle-Plastic Material. Part I and II, J. Eng. Mech., ASCE, 114(10), pp. 1672-1702., 1988.

11. Bazant, Z. P. and Pijaudier-Cabot, G. - Modeling of Distributed Damage by Nonlocal Continuum with Local Strains. 4th Int. Conf. on Numerical Methods in Fracture Mechanics, S. Antonio, ed. by A.R. Luxmore at all., pp. 411-432., 1988.

12. Bazant, Z. P. and Ozbolt, J. - Nonlocal Microplane Model for Fracture, Damage and Size Effect in Structures. Northwestern University - Civil Engineering Department, Report No, 89-10/498n, 1989.

13. Eligehausen, R. and Sawade, G. - 'A fracture mechanics based description of the pull-out behavior of head studs embedded in concrete', Fracture Mechanics of Concrete Structures - RILEM Report, Ed. L. Elfgren, Chapman and Hall, 1989, pp.263-280.

14. Sawade, G. - A contribution to the behavior of concrete in tension. Thesis in the preparation, Stuttgart University.

15. Elfgren, L.; Broms, C. E. and Johansson, H. - Anchor Bolts in Reinforced Concrete Foudations. Report No. 1980:36, University Lulea, 1980.

16. Furche, J. - Ausziehverzuche an Kopfbolcen mit kleinen Unterkopfflächen und Flachen Hinterschnittwinkeln. Report No. 9/4-88/1, Institut für Werkstoffe im Bauwesen,Universität Stuttgart, 1988.